Quantum Chemical Calculations of m-Toluidine and Investigation of Its Adsorption on Eggshells

Taner Kalaycı [1], Deniz Türköz Altuğ [2], Neslihan Kaya Kınaytürk [3*], Belgin Tunalı [3]

[1] Bandırma Onyedi Eylül University, Vocational School of Health Services, Bandırma, Balıkesir, Turkey

[2] Süleyman Demirel University, Faculty of Education, Department of Science Education, East Campus, 32260, Isparta, Turkey

[3] Burdur Mehmet Akif Ersoy University, Faculty of Arts and Sciences, Department of Nanoscience and Nanotechnology, Burdur, Turkey

Abstract

Aromatic nitro compounds, which have good water solubility, are one of the essential industrial pollutants, highly toxic and non-biodegradable, and adversely affect human health, aquatic life, and the environment. In this study, we have investigated the adsorption of m-toluidine on three types of eggshells characterized by FT-IR and FT-Raman spectroscopy. Also, the theoretical analysis of this harmful organic was determined using density functional theory on GAUSSIAN 09W software program. Molecular electrostatic analysis, Infrared and Raman vibrational bands, frontier molecular orbitals, and molecular geometry were investigated for this purpose. After the adsorption process, the NH_2 groups were observed at 3423-3347 cm^{-1} and 3433- 3350 cm^{-1} in CCJ-mT and C-CCJ/mT samples, respectively in FTIR spectrum. While these bands were not seen in CCJ-mT in the Raman spectrum, they were observed in C-CCJ-mT at 3429 and 3375 cm^{-1}. After adsorption, C-H bands were observed at 3216, 3036, 3013, 2978, 2919, 2865 cm^{-1} in CCJ/mT sample and at 3216, 3034, 3011, 2978, 2947, 2917, 2856 cm^{-1} in C-CCJ/mT sample. The C-C bands in the FTIR spectra of CCJ/mT and C-CCJ/mT samples were observed at 1591 and 1590 cm^{-1}, respectively, but they were not seen in the Raman spectrum after the adsorption.

Keywords: m-Toluidine, Quantum Chemical Calculations, Adsorption, Molecular Electrostatic Potential

m-Toluidin'in Kuantum Kimyasal Hesapları ve Yumurta Kabuklarına Adsorpsiyonunun İncelenmesi

Öz

Suda çözünürlüğü iyi olan aromatik nitro bileşikleri, temel endüstriyel kirleticilerden biridir, oldukça toksiktir ve biyolojik olarak parçalanamaz ve insan sağlığını, su yaşamını ve çevreyi olumsuz etkiler. Bu çalışmada, FT-IR ve FT-Raman spektroskopisi ile karakterize edilen üç tip yumurta kabuğu üzerinde m-toluidinin adsorpsiyonu nu araştırdık. Ayrıca GAUSSIAN 09W yazılım programında yoğunluk fonksiyonel teorisi kullanılarak bu zararlı organiğin teorik analizi yapılmıştır. Bu amaçla moleküler elektrostatik analiz, Kızılötesi ve Raman titreşim bantları, sınır moleküler orbitalleri ve moleküler geometri incelenmiştir. Adsorpsiyon işlemi sonrasında FTIR spektrumunda CCJ-mT ve C-CCJ/mT örneklerinde NH_2 grupları sırasıyla 3423-3347 cm^{-1} ve 3433- 3350 cm^{-1}'de gözlendi. Bu bantlar CCJ-mT nin Raman spektrumunda de görülmezken C-CCJ-mT' nin Raman spektrumunda 3429 ve 3375 cm^{-1}'de gözlendi. Adsorpsiyon sonrası CCJ/mT örneğinde 3216, 3036, 3013, 2978, 2919, 2865 cm^{-1}' de ve C-CCJ/'de 3216, 3034, 3011, 2978, 2947, 2917, 2856 cm^{-1}' de C-H bantları gözlendi. CCJ/mT ve C-CCJ/mT örneklerinin FTIR spektrumundaki C-C bantları sırasıyla 1591 ve 1590 cm^{-1}' de gözlemlenmiş, ancak adsorpsiyon işlemi sonrasında Raman spektrumunda görülmemiştir.

Anahtar Kelimeler: m-toluidin, Kuantum Kimyasal Hesaplamalar, Adsorpsiyon, Moleküler Elektrostatik Potansiyel

*Corresponding Author: nkinayturk@mehmetakif.edu.tr

Neslihan KAYA KINAYTÜRK, https://orcid.org/0000-0002-2170-1223
Taner KALAYCI, https://orcid.org/ 0000-0002-6374-2373
Deniz TÜRKÖZ ALTUĞ, https://orcid.org/ 0000-0002-1861-6263
Belgin TUNALI, https://orcid.org/0000-0003-0768-679X

1. Introduction

Today, recycling waste materials in the economy is a topic that attracts much attention and is being studied. The main reason why this subject attracts attention is that it is low cost and high gain. In addition, using natural waste material in any work also ensures minimized damage to the environment. Eggshells are a solid waste material, especially in the food industry. After the inner part of the egg is used, the shell parts are usually thrown away. However, these eggshells can now be used in many areas. On the one hand, it is used as a supplement due to the rich Ca content in its structure [1] [2] [3]; on the other hand, it is used as a biodiesel [4] [5]. It can even be used as a molecular adsorbent [6] [7] [8] while allowing it to adsorb heavy metals that cause environmental pollution due to the pores in its structure [9] [10]. There are studies in the literature about eggshells can be calcined and their ability to adsorb heavy metals or molecules can be increased [11] [12] [13] [14].

Three types of eggshells were used in this study. These were *Anser answer (AA), Denizli Hen (DH), and Coturnix Coturnix Japonica (CCJ)* eggshells. The reason for choosing these three samples is that the *AA* eggshell is very thick, the *DH* eggshell is of medium thickness, and the *CCJ* eggshell is thin. Figure 1 shows the consistency of these eggshells.

Figure 1. Photograph of the thickness of the eggshells (From left to right *AA, DH, and CCJ*)

m-Toluidine (m-methylaniline) is a simple aromatic amine compound bonded to the 1st carbon atom of the benzene ring with NH_2 (amine) and the 3rd carbon atom CH_3 (methyl) [15]. Its chemical formula is C_7H_9N. Its molecular structure is shown in Figure 2. m-Toluidine is used in dyestuffs, photochemicals, and antioxidants [16] [17]. In addition, an increase in m-toluidine was observed in smoking environments [17]. Aromatic amine group compounds are considered a compound in the severely destructive group for environmental and ecological balance [17, 18]. In addition, aniline and its derivatives can have a toxic and carcinogenic effect on human health, even if exposed in very low amounts [17] [19] [20].
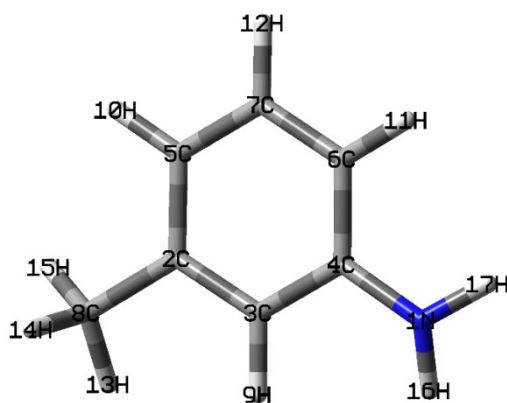
Figure 2. Molecular structure of m-Toluidine.

Apart from that, aromatic amine groups can easily mix with soil and water by decomposition of various insecticides, pesticides, and paint polyurethane classes. Thus, it can pose a threat to both the environment and human health [21]. Furthermore, in national and international environmental platforms, m-Toluidine is defined as a chemical threatening the environment and human life [22].

These aromatic amine groups can be easily analyzed by gas chromatography or liquid chromatography, but since high amounts of organic solvents will be used, they will be environmentally unfriendly methods [21]. Therefore, we used Raman and FTIR spectroscopic analysis in this study and obtained excellent results. These were also low cost, high analysis speed, low sample requirement, and environmentally friendly methods.

In this study, the adsorption properties of the m-toluidine molecule, which is densely present in the environment and may cause harm to human health on the one hand and environmental pollution on the other, were demonstrated by Raman and FTIR spectroscopy and theoretical calculations.

2. Materials and Methods

Eggshell samples AA*, DH, and CCJ* were obtained from Isparta University of Applied Sciences, Educational Research, and Application Farm. Eggshell samples were taken from the incubation wastes of the farm. m-Toluidine (mT) in liquid phase was bought from MERCK company. And they were used without purification. FTIR spectroscopic analysis was taken by JASCO FTIR 4700 Spectrometer.

2.1. Experimental Procedure

The cleaning procedure for eggshells was applied like the previous study, as in our last study [13]. They were put in a mortar. We used pure and calcinated powdered shells of each sample. The calcination process was performed by heating at 900°C for 2 hours. In the rest of the study, the calcination process is shown abbreviated with the letter "C." 0.5 gram of each sample treated

by 10 mL mT was used. They were shaken for 48 hours on stirring magnetic equipment. The samples were filtered and dried. It was then analyzed by FTIR spectroscopy.

2.2. Theoretical Details

Theoretical calculations had been done before another study [23].

3. Results and Discussion
3.1. Molecular Geometry

In this part of this work, bond lengths and angles for mT molecules were calculated to explain the molecular geometry. The optimized parameters of mT are presented in Table 1. The N1 atom in the amine molecule attached to the C4 atom in the benzene ring, which shows the characteristic geometry of the molecule, forms bonds with the H16 and H17 atoms, respectively. The bond length between N1-C4 is 1.411 Å. The bond lengths between N1-H16 and N1-H17 are 1.011 Å.

Table 1. Optimized parameters for mT

Atoms	Bond length (Å)	Atoms	Angle (°)	Atoms	Angle (°)
N1-C4	1.411	C4-N1-H16	120.04	C7-C6-H11	119.30
N1-H16	1.011	C4-N1-H17	120.04	C5-C7-C6	120.01
N1-H17	1.011	H16-N1-H17	119.93	C5-C7-H12	120.00
C2-C3	1.395	C3-C2-C5	120.00	C6-C7-H12	120.00
C2-C5	1.395	C3-C2-C8	120.02	C2-C8-H13	111.09
C2-C8	1.491	C5-C2-C8	119.98	C2-C8-H14	110.07
C3-C4	1.395	C2-C3-C4	120.00	C2-C8-H15	111.23
C3-H9	1.088	C2-C3-H9	119.98	H13-C8-H14	108.73
C4-C6	1.395	C4-C3-H9	120.02	H13-C8-H15	106.97
C5-C7	1.395	N1-C4-C3	120.02	H14-C8-H15	108.64
C5-H10	1.087	N1-C4-C6	119.98		
C6-C7	1.395	C3-C4-C6	120.00		
C6-H11	1.087	C2-C5-C7	120.00		
C7-H12	1.086	C2-C5-H10	120.72		
C8-H13	1.096	C7-C5-H10	119.29		
C8-H14	1.095	C4-C6-C7	120.00		
C8-H15	1.095	C4-C6-H11	120.71		

At the same time, the bond length of the N1 atom with both H16 and H17 forms the shortest bond in the molecule. In addition, the bond length between the C2 atom in benzene to which the methyl group is attached is 1.491Å, and this bond is the longest in the m-toluidine molecule. The bond lengths of H13, H14, and H15 atoms in the methyl group with C8 are equal and

1.095Å. The bond lengths between C3-H9, C5-H10, C6-H11, and C7-H12 atoms are 1.088, 1.087, 1.087, and 1.086Å, respectively. There are slight differences in the bond lengths between the carbon and hydrogen atoms. The reason for this can be explained as adding an amine molecule and methyl molecule to the benzene ring affects the C-H bond lengths in the benzene ring. The C-C bond lengths in the benzene ring are equal. Even though methyl and amine groups were added to the benzene molecule, it was observed that these additions did not disrupt the hexagonal structure of the benzene molecule.

When the CH_3 substitution was added to the C2 atom in the benzene ring, the angle between C3-C2-C5 was calculated to be 120.00°. The grades between the C8 atom attached to the C2 atom and the H13, H14, and H15 atoms were calculated as 111.09, 110.07, and 111.23°, respectively. The computed values here differ from each other. This difference is thought to be due to the geometry of the methyl group. The bond angles between the N1 atom attached to the C4 atom of the benzene ring and H16 and H17 were calculated as 120.04°. The angles between C-C-H in the benzene ring were estimated to be approximately 120° for each. When the C-C-C curves in the benzene ring were compared, it was seen that the angles in all the benzene rings had the same value. According to this result, it was seen that the angles between the carbon atoms in the ring were not affected even if methyl and amine groups were added to the benzene ring, just like the bond lengths.

3.2. Vibrational Analysis

In the first stage of this study, the %PED distributions of the theoretical vibrational bands of the mT molecule were calculated in detail. FTIR analysis was done experimentally, and the work of Puranik and Ramiah was used for the assignment of the Raman vibration bands [24]. Three eggshells were selected in the second stage (CCJ, AA, DH). Each of these eggshells was divided into two parts. While no treatment was applied to one part, calcination was applied to the other. mT adsorption was performed on untreated and treated eggshell samples, and then the vibration bands were reconsidered to prove the adsorption process. The intensities and detailed %PED assignments of the IR and Raman bands calculated by the B3LYP/6-311++G(d,p) method are given in Table 2. Since B3LYP vibrationalwavenumbers are known to be higher than the exper-imental wavenumbers, they were scaled down by auniform scaling factor of 0.983 for wavenumbers up to1700 cm^{-1} and of 0.958 for wavenumbers greater than1700 cm^{-1} [23]. The experimental FTIR and Raman vibrational bands of CCJ, mT/CCJ are presented in Figure 3.

3.2.1. NH₂ Vibration

Characteristic N-H vibrational bands are observed at 3500-3300 cm^{-1} [25]. The N-H asymmetric and symmetric vibration bands for mT were theoretically calculated at 3536 and 3443 cm^{-1}, respectively. These vibration bands were observed at 3450 and 3349 cm^{-1} in the experimental FTIR spectrum and 3455 and 3370 cm^{-1} in the Raman spectrum. N-H vibration bands were observed at 3423-3347 cm^{-1} and 3433-3350 cm^{-1} in the FTIR spectra of CCJ-mT

and C-CCJ/mT samples after the adsorption process. While these bands were not seen in CCJ-mT in the Raman spectrum, they were kept in C-CCJ-mT at 3429 and 3375 cm^{-1}.

3.2.2. C-H Vibration

C-H vibrational bands are observed at 3200-3000 cm^{-1} in aromatic and heteroatomic structures [26]. The C-H vibration bands of the investigated molecule were calculated as pure modes at 3069, 3055, 3044, 3033, 2991, 2967, and 2915 cm^{-1} with PED values of 93-97%. While these bands are observed at 3215, 3036, 3013, 2978, 2917, and 2857 in the IR spectrum, they are attributed to 3036, 2919, and 2865 cm^{-1} in the Raman spectrum. After adsorption, these bands were observed at 3216, 3036, 3013, 2978, 2919, and 2865 cm^{-1} in the CCJ/mT sample and at 3216, 3034, 3011, 2978, respectively 2947, 2917, 2856 cm^{-1} in C-CCJ/mT sample.

In-plane aromatic C-H bending vibrations occur as weak to moderate bands in the range of 1400-1000 cm^{-1} (C-H in the plane). In this study, these bands for mT were calculated at 1474, 1439, 1363, 1301, and 1150 cm^{-1}. It is assigned to 1467, 1432, 1376, 1311, 1170, and 1076 cm^{-1} in the experimental FTIR spectrum and 1431, 1377, 1157, 1077 cm^{-1} in the Raman spectrum. After adsorption, these bands are in the FTIR spectrum of the CCJ/mT sample at 1379, 1310, 1169, and 1080 cm^{-1}, and in the Raman spectrum at 1364, 1294, and1154 cm^{-1}. It was observed at 1469, 1364, 1312, 1292, 1170, 1090, and 1467, 1430, 1360, 1156 cm^{-1} in the FTIR and Raman spectrum, respectively of the C-CCJ/mT sample.

The out-of-plane C-H vibration bands are assigned to the 984-971 cm^{-1} range [27]. For the mT molecule, these vibration bands were observed at 995 and 928 cm^{-1} in the FTIR spectrum, while they were observed at 996-926 and 996-927 cm^{-1} in CCJ/mT and C-CCJ/mT samples, respectively.

3.2.3. C-C Vibration

In FTIR/ Raman Spectra, C=C and C-C vibration bands are observed in the range of 1650-1430 and 1614-1352 cm^{-1}, respectively [28]. While these bands were observed at 1588, 1491 cm^{-1} in the FTIR spectrum of the mT molecule, they were kept at 1585 cm^{-1} in the Raman spectrum. After adsorption, it was observed in the FTIR spectra of CCJ/mT and C-CCJ/mT samples at 1591 and 1590 cm^{-1}, respectively, but not in the Raman spectrum.
Similar assignments were made in AA/mT, DH/mT, C-AA/mT, C-DH/mT samples. Details are presented in the attached file.
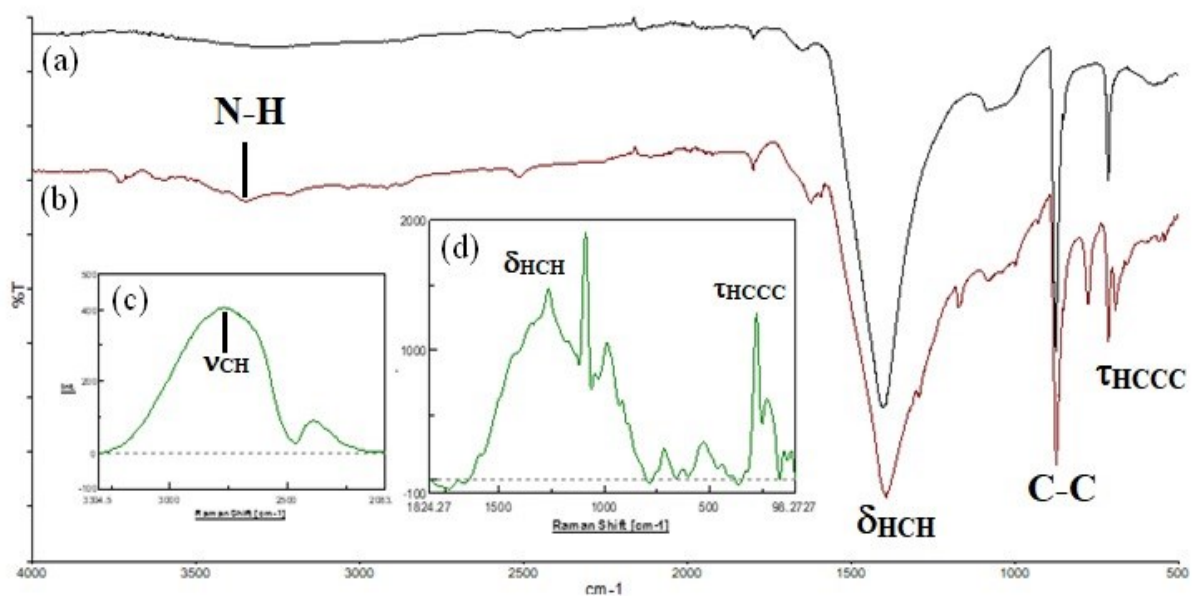
Figure 3. (a) FTIR spectrum of CCJ (b) FTIR spectrum of mT/CCJ (c) Raman spectrum of mT/CCJ in the range of 3500-2080 cm^{-1} (d) Raman spectrum of mT/CCJ in the range of 1800-96 cm^{-1}

Table 2. Detailed assignments of experimental and theoretical wavenumbers (cm^{-1}) of mT, CCJ/mT, C-CCJ/mT, along with potential energy stribution.

mT DFT	Scaled	I_{IR}	I_R	Exp. mT		CCJ/mT		C-CCJ/mT		Assignment
				IR	Raman [*]	IR	Raman	IR	Raman	
3664	3536	15.01	57.89	3450	3455	3423w		3433 w	3429 w	ν_{NH} (100)
3567	3443	16.74	205.88	3349	3370	3347w		3350 w	3375 w	ν_{NH} (100)
3180	3069	17.34	215.7	3215		3216w		3216		ν_{CH} (93)
3165	3055	21.36	65.35	3032		3036w		3034 w		ν_{CH} (93)
3154	3044	4.93	72.89	3017	3011	3013 vw		3011 w		ν_{CH} (93)
3143	3033	20.92	80.18	2982		2978 vw		2978 vw		ν_{CH} (99)
3099	2991	17.65	62.20	2950				2947 vw		ν_{CH} (96)
3074	2967	20.36	83.03	2917	2915	2919w		2917 w		ν_{CH} (95)
3020	2915	31.41	242.30	2857	2869	2865w	2807	2856 w	2810 s	ν_{CH} (97)
1662	1604	152.59	22.35	1628	1612			1621 m		δ_{HNH} (70)+ τ_{HNCC} (10)
1646	1589	53.67	17.85	1588	1585	1591sh	1583 w	1590sh		ν_{CC} (41)+ δ_{HNH} (12)
1627	1570	25.45	9.09	1491	1480			1493 m		ν_{CC} (41)+ δ_{CCC} (28)
1527	1474	38.28	1.64	1467				1469 m	1467sh	δ_{HCC} (47)+δ_{CCC} (15)
1491	1439	6.95	9.97	1432	1431		1429sh		1430 w	δ_{HCH} (71)+ τ_{HCCC} (21)
1412	1363	1.04	14.39	1376	1377	1379 sh	1364 s	1364sh	1360	δ_{HCH} (91)
1348	1301	4.58	1.19	1311		1310 vw		1312 sh		δ_{HCC}(49)+ν_{CC} (30)
1339	1292	9.42	2.15	1292	1295	1291 m	1294 sh	1292 m	1291 sh	ν_{CC} (32)+ δ_{HNC} (25)
1192	1150	2.14	1.91	1170	1157 w	1169w	1154 s	1170 m	1156 s	δ_{HCC}(63)+ν_{CC} (12)
1131	1092	2.13	3.62	1076	1077 s	1080		1090	1085 s	δ_{HCC}(30)+ δ_{HNC} (25)+ ν_{CC} (19)
1092	1054	1.98	1.34	1036		1038	1035	1053		δ_{HNC} (34)+ ν_{CC} (26)+ δ_{HCC}(10)
1058	1021	8.33	1.69	995		996 w		996 w		τ_{HCCC}(62)
1009	974	2.22	42.71		968 s	963 sh		961 sh		δ_{CCC} (57)+ ν_{CC} (35)
973	939	0.03	0.22	928	927 sh	926 w		927 w		τ_{HCCC}(88)
860	830	6.94	0.33	773	776	773 m		774 m	775 w	τ_{HCCC}(64)
747	721	0.54	19.15		736	711 m		712 m	735 w	δ_{CCC}(48)+ν_{CC} (26)
702	678	18.84	0.19	663		669 sh		666 sh		τ_{HCCC}(63)+γ_{CCCC}(12)

ν=stretching; δ=deformation (bending); τ=torsion; vs= very strong; s=strong; m=medium; w=weak; vw= very weak; sh=shoulder, PED: Potential energy distribution

* [24]

3.3.   Molecular electrostatic potential surface (MEP) analysis

Molecular electrostatic potential surface maps (MEP) reveal the charge distribution of molecules along with different charge regions. It is convenient to guess the charge distribution, electrophilic feature, molecular behavior, activity, and details of hydrogen bonding [29]. In addition, MEP maps pave the way for new chemical synthesis methods by clarifying active sites between intramolecular bonds. The color codes of the electrostatic potential surface map are depicted in Figure 4. The decrease in potential continues in the order of blue>green>yellow>orange>red [30] [31].
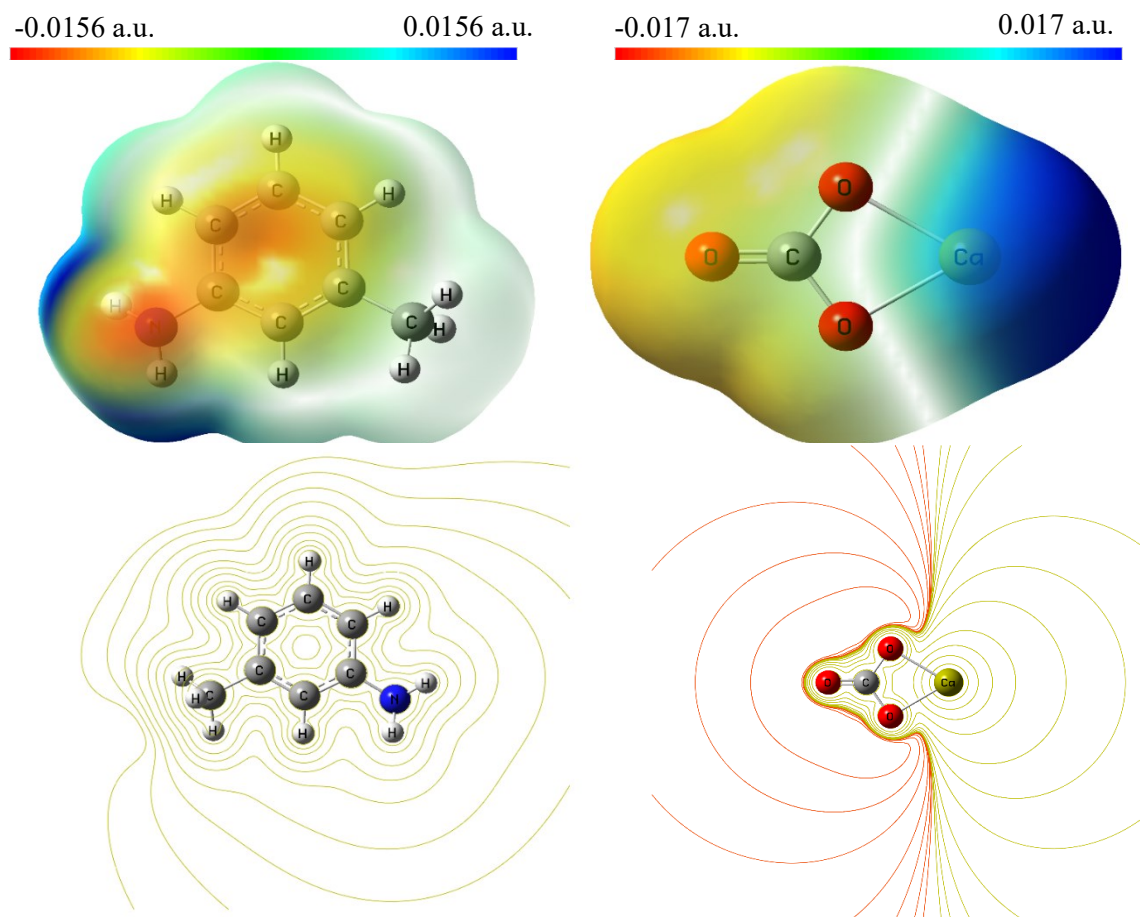
Figure 4. Molecular electrostatic potential mapped of m-Toluidine and $CaCO_3$

In the MEP map of the molecule, the electron deficient region is coded in blue, and the region with high electron density is coded in red. Regions with the most positive and negative potential for m-Toluidine are 0.156 to -0.156 a.u. The relatively red region in the center of the ring is the most electronegative but is localized to the N atom. Blue region is the most nucleophilic region, a concentrated Hydrogen atom in NH_2. On the other hand, the region with the most positive to most negative potential is between 0.017 to -0.017 a.u. for $CaCO_3$. The most nucleophilic region is concentrated on the Calcium atom and is coded in blue, while the most electronegative region is coded in red and located on the O atoms. The graph of Mulliken' s atomic charges is given in Figure 5.
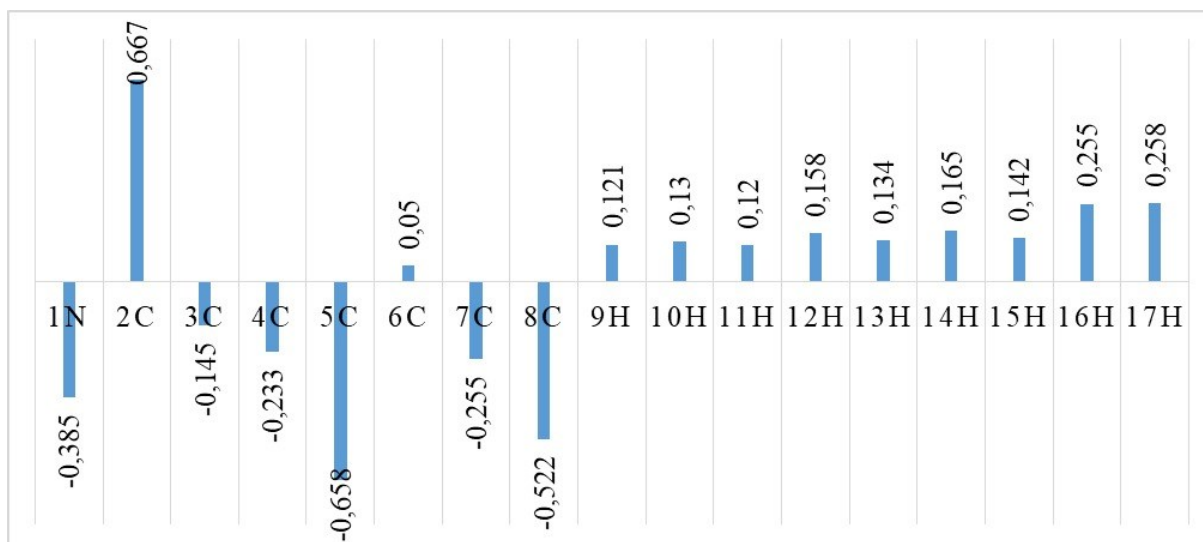
Figure 5. Mulliken Atomic Charges of m-Toluidine

Mulliken population analysis supplements MEP analysis in identifying electronegative sites within a molecule. MEP and Mulliken population analysis are very convenient methods to explain the reactive behavior of all chemical systems in electrophilic and nucleophilic reactions. Detailed Mulliken population analysis for the title molecule is shown in Figure 5. It is seen that the results are in good agreement with the MEP results and among themselves.

3.4. Frontier molecular orbitals (FMOs) and chemical activity

HOMO (Highest Occupied Molecular Orbital) and LUMO (Lowest Unoccupied Molecular Orbital) energies are essential properties in theoretical calculations. HOMO and LUMO surface images and the calculated parameters are given in Figure 6 and Table 3, respectively.
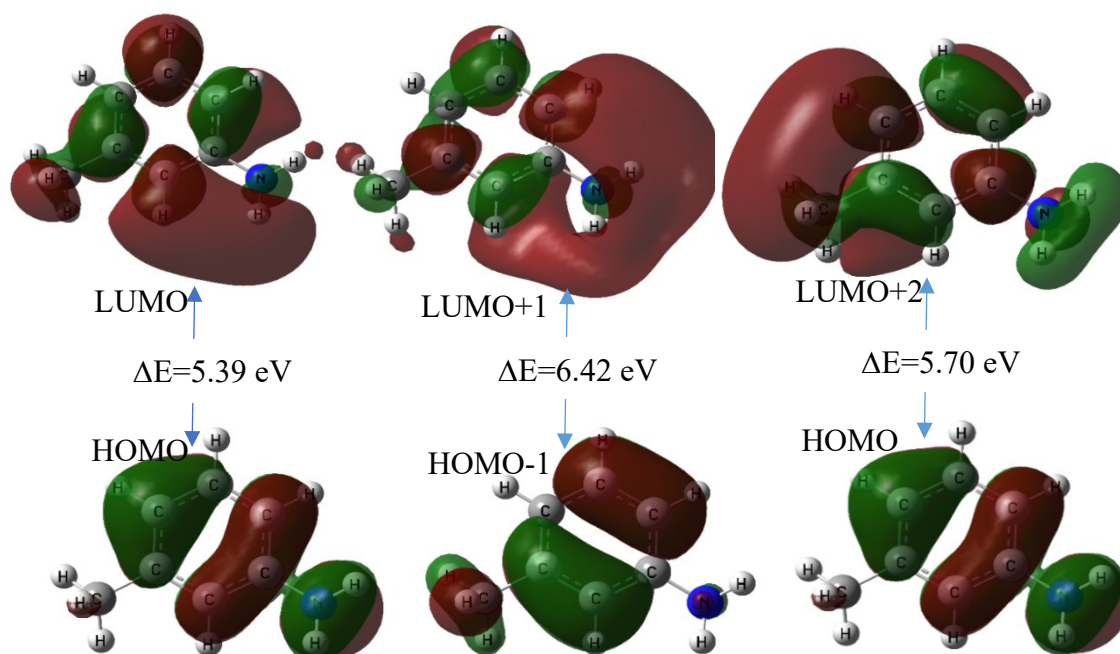
Figure 6. Highest occupied molecular orbital and lowest unoccupied molecular orbital plot of mT

Table 3. Calculated energy values of mT

Parameters	mT (eV)
E_{HOMO}	-5.670
E_{LUMO}	-0.280
ΔE	5.390
Ionization potential (I)	5.670
Electron affinity (A)	0.280
Electronegativity (χ)	2.980
Chemical potential (μ)	-2.980
Chemical hardness (η)	2.700
Chemical softness (s)	0.180
Electrophilic index (w)	1.640
Maximum load transfer parameter (ΔN max)	0.550

m: meta form of toluidine; eV: electron-Volt; E_{HOMO}: highest occupied molecular orbital energy; E_{LUMO}: lowest unoccupied molecular orbital energy; ΔE: energy differences between HOMO and LUMO

Results show that mT has high hardness and low softness parameters due to increased energy gaps. These show that this molecule has low chemical activity and high kinetic stability, and it can therefore be concluded that it is pretty stable. High hardness and common softness values indicate less intermolecular charge transfer and low polarity. HOMO energy is calculated as -5.670 eV for mT. LUMO energy is calculated as -0.280. Also, the energy gap is calculated as 5.390 eV. This low HOMO–LUMO energy gap shows that the charge transfer occurs in mT. Electronegativity (χ) and chemical hardness (η) can be calculated as used in the frontier molecular orbital energies [32]. In a molecule, the electron will be transferred from low w to high w (electrons flow from high chemical potential to low chemical potential). In the molecule, χ value is obtained as 2.980 eV. From the HOMO and LUMO energies, the η value is defined as 2.700 eV for mT.

3.5. AFM Analyses

When the eggshells of CCJ, DH and AA are compared to each other, AFM images reveal that the pore sizes are different. When Figure 7 is examined, it is seen that CCJ has a small circular pore structure and AA has a channel-shaped pore structure. AFM images show that the CCJ eggshell has the maximum number of pores per unit surface. Since the mT molecule is a relatively small molecule, it can be said that it easily settles into these small pores. For this reason, it was thought that adsorption was positively affected.
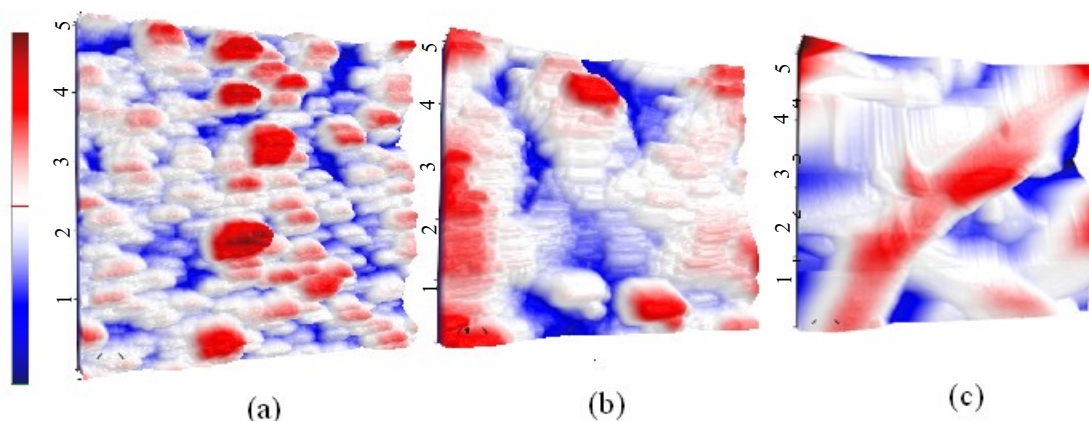
Figure 7. AFM Images and region histogram of Eggshell Sample (a) CCJ (b) DH (c) AA

4. Conclusion

Theoretical calculations give valuable information about bond lengths. mT molecule shows slight differences in bond lengths between C and H atoms. Even though methyl and amine groups were added to the benzene molecule, it was observed that these additions did not disrupt the hexagonal structure of the benzene molecule. According to this result, it was seen that the angles between the carbon atoms in the ring were not affected even if methyl and amine groups were added to the benzene ring, just like the bond lengths. It can be concluded that the adsorption was noticed more strongly in the CCJ type among the three eggshell types. The most distinctive feature of CCJ is its thin crust and small pores. mT molecule is a relatively small molecule. For mT, it is possible to say that as the results, mT settles in tiny pores comfortably. Another conclusion, the adsorption process can be viewed on carbonized eggshells dominantly. The vibrational frequencies were almost the same in FTIR spectra after adsorption on eggshells; these results indicated that physical adsorption had taken place. 2C has a positive Mulliken atomic charge compared to other Carbon atoms in mT. The substitute CH_3 group is linked at 2C in mT. This indicates that the 2C has a more nucleophilic behavior. mT has high hardness and low softness parameters due to its high energy gaps. These indicate that this molecule has low chemical activity and high kinetic stability; therefore, it can be concluded that it is pretty stable. The high stability feature of the mT molecule shows the unwillingness of any chemical reaction. This property is the demonstration of physical adsorption on eggshells. In addition, $CaCO_3$, the eggshell's primary content, affects the electrical charge attraction on the surface to adsorb the mT molecule. Mulliken's atomic charge distribution supports the idea.

Author Contributions

Taner Kalaycı; Investigation, Original Draft Writing, Material/Instrument Supply

Deniz Türköz Altuğ: Investigation, Original Draft Writing, Material Supply

Neslihan Kaya Kınaytürk: Investigation, Computational and Experimental Analyses, Original Draft Writing, Visualization, Review and Editing,

Belgin Tunalı: Investigation, Experimental Analyses, Original Draft Writing, Material/Instrument Supply, Supervisor.

Ethics in Publishing

There are no ethical issues regarding the publication of this study.

Acknowledgments

References

[1] Waheed, M., Butt, M. S., Shehzad, A., Adzahan, N. M., Shabbir, M. A., Suleria, H. A. R., Aadil, R. M. (2019). "Eggshell calcium: A cheap alternative to expensive supplements", *Trends in Food Science & Technology*, 91, 219-230.

[2] Gaonkar, M., Chakraborty, A. P. (2014) "Application of eggshell as fertilizer and calcium supplement tablet", *International journal of innovative research in science, engineering and technology,* 5(3), 3520-3525.

[3] Schaafsma, A., Van Doormaal, J. J., Muskiet, F. A., Hofstede, G. J., Pakan, I., Van der Veer, E., (2002). "Positive effects of a chicken eggshell powder-enriched vitamin–mineral supplement on femoral neck bone mineral density in healthy late post-menopaus Dutch women", *British Journal of Nutrition,* 87(3), 267-275..

[4] Kirubakaran, M., Selvan,V. A. M. (2021). "Experimental investigation on the effects of micro eggshell and nano-eggshell catalysts on biodiesel optimization from waste chicken fat", *Bioresource Technology Reports,* 14(100658), 1-10.

[5] Kavitha, V., Geetha V., Jacqueline, P. J. (2019). "Production of biodiesel from dairy waste scum using eggshell waste", *Process Safety and Environmental Protection,* 125, 279-287.

[6] Kınaytürk, N. K., Tunalı, B., Türköz Altuğ, D. (2021). "Eggshell as a biomaterial can have a sorption capability on its surface: A spectroscopic research", *Royal Society Open Science,* 8(6), 1-14.

[7] Muhammad, I. M., El-Nafaty, U. A., Abdulsalam, S., Makarfi, Y. I. (2012). "Removal of oil from oil produced water using eggshell", *Civil and Environmental Research,* 2(8), 52-63.

[8] Jendia, A. H., Hamzah, S., Abuhabib, A. A. El-Ashgar, N. M. (2020) "Removal of nitrate from groundwater by eggshell biowaste", *Water Supply,* 20(7), 2514-2529.

[9] Rahmani-Sani, A., Singh, P. Raizada, P. E. Lima, C. Anastopoulos, I. D., Giannakoudakis, A., Sivamani, S., Dontsova T., Hosseini-Bandegharaei, A. (2020). "Use of chicken feather and eggshell to synthesize a novel magnetized activated carbon for sorption of heavy metal ions", *Bioresource Technology,* 297(122452), 1-9.

[10] Lin, T. Y., Chai, W. S. Chen, S. J., Shih, J. Y., Koyande, A. K., Liu, B. L., Chang, Y. K. (2021). "Removal of soluble microbial products and dyes using heavy metal wastes decorated on eggshell", *Chemosphere,* 270(128615), 1-12.

[11] Lee, J. I., Kim, J. M., Yoo, S. C., Jho, E. H., Lee, C. G., Park, S. J. (2022). "Restoring phosphorus from water to soil: Using calcined eggshells for P adsorption and subsequent application of the adsorbent as a P fertilizer", *Chemosphere,* 287(132267), 1-10.

[12] Eletta, O. A. A., Ajayi, O. A., Ogunleye, O. O., Akpan, I. C. (2016). "Adsorption of cyanide from aqueous solution using calcinated eggshells: Equilibrium and optimisation studies", *Journal of Environmental Chemical Engineering,* 4(1), 1367-1375.

[13] Türköz Altuğ, D. Kaya Kınaytürk, N., Kalaycı, T., Tunalı, B. (2022). "Heavy Metal Adsorption with Eggshell of Phasianus Colchicus", *Süleyman Demirel Üniversitesi Fen Edebiyat Fakültesi Fen Dergisi=Süleyman Demirel University Faculty of Arts and Science,* 17(1), 230-241.

[14] Eskikaya, O., Gun, M., Bouchareb, R., Bilici, Z., Dizge, N., Ramaraj, R., and Balakrishnan, D. (2022). "Photocatalytic activity of calcined chicken eggshells for Basic Red 2 and Reactive Red 180 decolorization", *Chemosphere,* 304(135210), 1-10.

[15] Allan, J. R., Paton, A. D. (1993). "Preparation, structural characterisation, thermal and electrical studies of complexes of cobalt, nickel and copper with m-toluidine", *Thermochimica acta,* 214(2), 235-241.

[16] [Online]. Available: https://www.chemicalbook.com/ChemicalProductProperty_EN_CB4277541.htm.

[17] Palmiotto, G., Pieraccini,G., Moneti, G., Dolara, P. (2001). "Determination of the levels of aromatic amines in indoor and outdoor air in Italy". *Chemosphere*, 43(3), 355-361.

[18] Thippeswamy, MS, Naik L., Maridevarmath, C. V., Malimath G. H. (2022). "Interactions of Environmental Pollutant Aromatic Amines With Photo Excited States of Thiophene Substituted 1, 3, 4-Oxadiazole Derivative: Fluorescence Quenching Studies", *Journal of Fluorescence,* 32, 1543–1556.

[19] Aktaş Şüküroğlu, A., Burgaz, S. (2018). "Occupational Exposure to the Chemicals in Hairdressing Salons and Health Risk", *Turkish Bulletin of Hygiene and Experimental Biology,* 75(2), 195-212.

[20] Johansson, G. M., Jönsson, B. A., Axmon, A. C., Lindh, H., Lind, M. L., Gustavsson, M., Broberg, K., Boman, A., Meding, B., Lidén, C., Albin, M. (2015). "Exposure of hairdressers to ortho-and meta-toluidine in hair dyes" *Occupational and Environmental Medicine,* 72(1), 57-63.

[21] Zhou, Q., Jiang, G., Liu, J., Cai, Y. (2004). "Combination of microporous membrane liquid–liquid extraction and capillary electrophoresis for the analysis of aromatic amines in water samples", *Analytica chimica acta,* 509(1), 55-62.

[22] Pinheiro, H. M., Touraud, E., Thomas, O. (2004). "Aromatic amines from azo dye reduction: status review with emphasis on direct UV spectrophotometric detection in textile industry wastewaters", *Dyes and pigments,* 61(2), 121-139.

[23] Kaya Kınaytürk, N., Oturak, H. (2016). "Identification of Structural and Spectral Features of 2-Amino 4-Chlorobenzoic Acid and 4-Amino 2-Chlorobenzoic Acid: A Comparative Experimental and DFT Study", *Acta Physica Polonica Series a,* 130(1), 276-281.

[24] Puranik, P., Ramiah, K. (1961). "Raman and infra-red spectra of amines, Toluidines andpara-amino-acetophenone", *Proceedings of the Indian Academy of Sciences - Section A,* 54, 146–154.

[25] Mohammed, T., Soliman, U., Hanafy, A., Hassan, A. M. (2008). "Conformational stability, barriers to internal rotation of 2-aminothiophenol (d0 and d3): A combined

vibrational and theoretical approach", *Journal of Molecular Structure: THEOCHEM,* 865(1-3), 14-24.

[26] Zochedh, A., Priya, M., Shunmuganarayanan, A., Thandavarayan, K., Sultan, A. (2022). "Investigation on structural, spectroscopic, DFT, biological activity and molecular docking simulation of essential oil Gamma-Terpinene", *Journal of Molecular Structure,* 1268, 133651.

[27] Hony, S., Van Kerckhoven, C., Peeters, E., Tielend, A., Hudgins, D., Allamandola, L. (2001). "The CH out-of-plane bending modes of PAH molecules in astrophysical environments", *Astronomy and Astrophysics,* 370(3), 1030 -1043.

[28] Altun, A., Gölcük, K., Kumru, M. (2003), "Theoretical and experimental studies of the vibrational spectra of m-methylaniline", *Journal of Molecular Structure: THEOCHEM,* 625(1-3), 17-24.

[29] Berrah, F., Boursas, F., Bouacida, S., Ouannassi, F. (2020). "Structural, Spectroscopic and Thermal Characterizations Combined with DFT Calculations and Hirshfeld Analysis of a Novel Hydrogen-Bonded Complex: P-Phenylenediammonium Dinitrate", *Journal of Molecular Structure,* 1205, 127624.

[30] Chaudhary, J., Mittal,V., Mishra, S., Daiya, A., Chowdhury, R., Laskar, I. R., Roy, R. K." (2020). A New Aggregation Induced Emission Active Halochromic White Light Emissive Molecule: Combined Experimental and Theoretical Study", *The Journal of Physical Chemistry,* 124(28), 15406-15417.

[31] Kaya Kınaytürk, N., Kalaycı, T. Tunalı, B. (2021). "Experimental and computational investigations on the molecular structure, vibrational spectra, electronic properties, and molecular electrostatic potential analysis of phenylenediamine isomers" *Spectroscopy Letters,* 54(9), 693-706.

[32] Keçel-Gündüz, S., Bıçak, B., Çelik, S., Akyüz, S., Özel, A. (2017) "Structural and spectroscopic investigation on antioxidant dipeptide, l-methionyl-l-serine: A combined experimental and DFT study". *Journal of Molecular Structure*, 1137, 756-770.